Marketa Ryvolova[1,2,3]
David Hynek[1]
Helena Skutkova[4]
Vojtech Adam[1,3]
Ivo Provaznik[4]
Rene Kizek[1,3]

[1]Department of Chemistry and Biochemistry, Faculty of Agronomy, Mendel University in Brno, Brno, Czech Republic
[2]Department of Microelectronics, Faculty of Electrical Engineering and Communication, Brno University of Technology, Brno, Czech Republic
[3]Central European Institute of Technology, Brno University of Technology, Brno, Czech Republic
[4]Department of Biomedical Engineering, Faculty of Electrical Engineering and Communication, Brno University of Technology, Brno, Czech Republic

Received June 13, 2011
Revised July 11, 2011
Accepted July 12, 2011

Research Article

Structural changes in metallothionein isoforms revealed by capillary electrophoresis and Brdicka reaction

Metallothionein (MT) as a potential cancer marker is at the center of interest and its properties, functions and behavior under various conditions is intensively studied. In the present study, two major mammalian MT isoforms (MT-1 and MT-2) were separated using capillary electrophoresis (CE) coupled with UV detector in order to describe their basic behavior. Under the optimized conditions, the separation of both isoforms was enabled as well as estimation of detection limits as subunits and units of ng per μL for MT-2 and MT-1, respectively. Further, the effects of thermal treatment and the presence of denaturing agent such as urea on MT-1 and MT-2 isoforms were studied by CE-UV. Thermal treatment caused an increase in the signals of both isoforms. A new parameter called precipitation rate has been defined based on this finding. This parameter can be expressed as a slope of the linear regression of the time dependency curve recalculated on the MT concentration. The thermal precipitation rate for MT-1 and MT-2 was determined as 1.1 and 0.9 ng of MT/min, respectively. The chemical precipitation rate calculated from the linear regression for both isoforms provided the same value of 0.25 ng of MT/min. The results were confirmed by manual spectrometric measurements and by differential pulse voltammetry Brdicka reaction. Based on these results, a model of MT behavior under the conditions studied was suggested.

Keywords:
Brdicka reaction / Cancer / CE / Denaturation / Electrochemistry / Isoforms / Metallothionein
DOI 10.1002/elps.201100312

1 Introduction

Metallothioneins (MTs) are a group of small molecular mass proteins (6–10 kDa) rich in amino acid cysteine [1–3]. Four mammalian MT isoforms (MT-1, MT-2, MT-3 and MT-4) and 13 MT-like human proteins have been identified. MT-1 and MT-2 are present almost in all types of soft tissues [4], MT-3 is expressed mostly in brain tissue but also in the heart, kidneys, and reproductive organs [5] and MT-4 gene was detected in epithelial cells [6]. MT ensures a wide range of functions in the organism including metal homeostasis, heavy metal detoxification, maintenance of the redox pool, radical scavenging and/or regulation of transcription [7–9]. Based on the fact that tumor cell alter many biochemical pathways including those responsible for maintaining of metal ions, it is not surprising that these proteins attract scientists as potential tumor disease marker on one side and as targets for certain treatment strategies on the other side [10–13]. However, roles of MT isoforms in these pathological processes remain still unclear. Therefore, investigation of properties and behavior of these proteins – total quantification as well as detection of single isoforms under various conditions – is of great importance [14–17].

To study MT, there have been suggested numerous methods and techniques based on various physico-chemical mechanisms [18, 19]. There are both advantages and disadvantages in each method, but one of them belongs to those few enabling to separate single MT isoforms and to detect them sensitively – CE [20–24]. In the work of Kawata et al. [25] also the diagnostic potential of MT isoforms was discussed. The detection of the protein is commonly carried out with UV detector at 214 or 254 nm; however, there is a limitation since concentrations of MT are commonly app. 1 mg/mL due to poor absorption characteristics of these proteins. Mass spectrometers including those connected with inductively coupled plasma ionization can be also used for detection of MT [26–28].

In this study, two major isoforms were separated using CE coupled with UV detector in order to describe their basic behavior. Further, the influence of thermal treatment and the presence of denaturing agent such as urea on MT-1 and MT-2 isoforms were studied by CE-UV. The results obtained

Correspondence: Dr. Rene Kizek, Department of Chemistry and Biochemistry, Mendel University in Brno, Zemedelska 1, CZ-613 00 Brno, Czech Republic
E-mail: kizek@sci.muni.cz
Fax: +420-5-4521-2044

Abbreviation: MT, metallothionein

Colour Online: See the article online to view Figs. 2–8 in colour.

were compared with those measured by differential pulse voltammetry Brdicka reaction [29–31] and UV spectrometry and new constant of precipitation was defined.

2 Materials and methods

2.1 Chemicals

Rabbit liver MT isoforms (MT-1, MT-2) sodium borate and urea were purchased from Sigma-Aldrich (USA) in ACS quality. Other chemicals used were also purchased from Sigma-Aldrich unless stated otherwise. The stock standard solutions of MT (1 mg/mL) was prepared with ACS water and stored in the dark at −20°C. Working standard solutions were prepared daily by dilution of the stock solutions with ACS water. All other solutions used were prepared in MiliQwater. Deionized water underwent demineralization by reverse osmosis using the instrument Aqua Osmotic 02 (Aqua Osmotic, Tisnov, Czech Republic) and then subsequently purified using Millipore RG (Millipore Corp., USA, 18 MΩ) – MiliQ water. The pH value and conductivity was measured using inoLab Level 3 (Wissenschaftlich-Technische Werkstätten GmbH; Weilheim, Germany).

For chemical denaturation, 0.1 mg/mL MT was prepared in 7.5 M urea and time dependency was measured by DPV and CE. Thermal denaturation was carried out in the thermomixer (Eppendorf Thermomixer Comfort, USA). The sample was heated for 99°C for 20 min if not stated otherwise.

2.2 Bioinformatics analysis

The phylogenetic tree was created based on the evolutionary similarities of seven MT sequences from rabbit liver. BIONJ method was used as a suitable technique for this type of data [32]. The pairwise distance of the sequences was determined using Jukes–Cantor evolution model. Sequences were aligned for the same size using global alignment with following parameters: score matrix BLOSUM80, inserted gaps $G_i = 2$, extended gaps $G_e = 0$ [33]. Subsequently, the phylogenetic tree was evaluated by bootstrapping of 100 pseudo-samples. The entire phylogenetic analysis including statistical evaluation and alignment was performed using application created in Matlab software with bioinformatic toolbox. The representative sequence logo was created from the same data set. The change fraction was expressed in percentage of the ratio of occurrence each amino acid on certain position. Acidic and basic amino acids were color coded: neutral-black, acidic-red, basic-blue. Logo was created in professional application WebLogo3 [34].

2.3 Spectrometric measurements

Spectrophotometric analyses were performed using manual spectrophotometer Specord 210 (Analytic Jena, Germany). The sample was placed into the low-volume (40 μL) quartz cell with optical path length of 1 cm. UV range of spectra was recorded in operating software (Analytic Jena, Germany).

2.4 Differential pulse voltammetry – Brdicka reaction

Differential pulse voltammetry (DPV) Brdicka reaction measurements were performed with AUTOLAB Analyzer (EcoChemie, Netherlands) connected to VA-Stand 663 (Metrohm, Switzerland), using a standard cell with three electrodes. A hanging mercury drop electrode (HMDE) with a drop area of 0.4 mm^2 was employed as the working electrode. An Ag/AgCl/3M KCl electrode served as the reference electrode. Glassy carbon electrode was used as the auxiliary electrode. For smoothing and baseline correction the software GPES 4.9 supplied by EcoChemie was employed. The Brdicka supporting electrolyte containing 1 mM $Co(NH_3)_6Cl_3$ and 1 M ammonia buffer ($NH_3(aq)$+ NH_4Cl, pH 9.6) was used and changed per each measurement. The DPV parameters were as follows: initial potential of −0.7 V, end potential of −1.75 V, modulation time 0.057 s, time interval 0.2 s, step potential 2 mV, modulation amplitude −250 mV, time of accumulation 240 s.

2.5 CE

All analyses were carried out using CE instrument from Beckman Coulter (P/ACE 5500, USA) equipped with UV absorbance detector. Separations were performed in an uncoated fused-silica capillary (Polymicro Technologies, USA) with an internal diameter of 75 μm and external diameter of 375 μm. The total length of the capillary was 57 cm and the effective length was 50 cm. The capillary was flushed with 0.1 M NaOH for 5 min and with background electrolyte for 10 min prior to the first use. The capillary was rinsed for 2 min with background electrolyte before each run to obtain stable and repeatable measurements. Sample was injected hydrodynamically by pressure of 3.4 kPa applied for 20 s. Separation voltage was set to 15 kV. Sodium borate buffer (20 mM, pH 9.5) was used as a background electrolyte (BGE). The signal was registered at 214 and 254 nm.

3 Results and discussion

As mentioned above, four mammalian isoforms of MT have been identified. MT-1 and MT-2 are the most abundant one. It is also most probable that they might be associated with various pathological processes. Therefore, this study focused primarily on these two isoforms. Since rabbit MT are commonly used as a model compound for analytical and biochemical investigation, the present work is focused on

bioinformatics analysis of rabbit MT structures based on the data obtained from bioinformatics database.

3.1 Bioinformatics analysis

Data obtained from the protein database (UniProtKB) were analyzed using bioinformatics tools employing the Matlab software. The evolutionary relationships between isoforms were evaluated by construction of diagrams (phylogenetic trees) based upon similarities and differences in their physical and/or biochemical characteristics. Based on the phylogenetic tree (Fig. 1) seven proteins (MT-1A, MT-2A, MT-2B, MT-2C, MT-2D, MT-2E and E2GJC7) were included into the group of MT-1 and MT-2 proteins of rabbit MT isoforms. It can be concluded from the diagram that sequences are so similar that their statistic value dropped under 90% only in the case of the root node. The topology of the tree shows significant division into clusters with the identical sequence length. This is caused by the fact that amino acid substitutions are sporadic and therefore the highest statistical weight in similarity evaluation is given to the insertions and deletions occurring during evolution. Basic bioinformatics data such as protein ID, name, number of amino acids, molecular weight and theoretical p*I* are summarized in Table 1.

The 3D structure of the MT is shown in Fig. 2A. It is demonstrating the ability of the protein to bind up to seven metal ions (Zn, Cd, Cu, Hg, Pb, Au and Bi) via the sulfhydryl group of cysteine [35]. Aligned amino acid sequences are listed in Fig. 2B to express the similarity in amino acid composition. Differences of constituent forms come mainly from post-translational modifications, type of incorporated metal ion and speed of degradation. Despite the physicochemical similarity of the forms, their roles and occurrence in tissues vary significantly. Representative logo (Fig. 2C) illustrates the probability of certain amino acid to occur at certain position. The probability increases with the size of the letter. To highlight the electrophoretic properties, the number of acidic and basic amino acid as well as theoretical p*I* for each isoform and sub-isoform is plotted in Fig. 2D. The negative charge is distributed by asparagic and glutamic acid (p*K*a of the residues are 3.9 and 4.3, respectively). Basic amino acids are represented by lysine and arginine in the case of MT-2E and MT-2D sub-isoform. The p*K*a of lysine residue is 10.5 and 12.5 for arginine. In this study, pH of the background electrolyte was 9.5 and therefore basic amino acids are non-charged and do not contribute significantly to the net charge of the protein. These results are in good agreement with Trnkova et al., where authors found negligible electroactivity of MT under the presence of borate buffer used as background electrolyte in this study due to non-charged basic amino acids [36]. The theoretical p*I* of studied MT-1 and MT-2 is distributed in a very narrow range from 8.23 to 8.38. Due to the absence of aromatic amino acids as typical structural feature of MTs, the absorbance in UV region is closely connected with the presence of amino acid cysteine, which is highly abundant in these proteins as can be seen in Fig. 3. Cysteine and its ability to give a peak can be also used for studying metal-thiolate clusters in MT [24, 37]. The results shown in Fig. 3 indicate that MT (0.1 mg/mL) isoforms can be detected using UV spectrometry. Thus, the CE-UV was utilized for detection of both isoforms in the following part of the study.

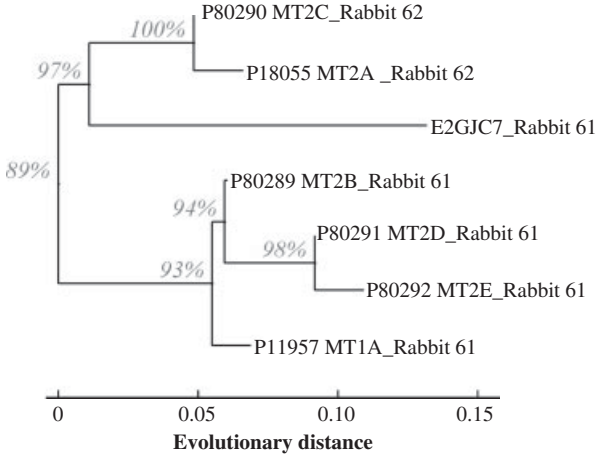

Figure 1. Phylogenetic tree for rabbit MT-1 and MT-2 isoforms and sub-isoforms. Sequences were aligned for the same size using global alignment with parameters: score matrix BLOSUM80, inserted gaps $G_i = 2$, extended gaps $G_e = 0$. Subsequently, the phylogenetic tree was evaluated by bootstrapping of 100 pseudo-samples. The entire phylogenetic analysis including statistical evaluation and alignment was performed using an application created in the Matlab software with the bioinformatic toolbox.

3.2 CE analysis

As noted previously, a variety of CE methods employing wide range of electrolytes [38–40] as well as electrolyte modifiers [41, 42] and capillary surface coatings [23, 43] has been used for detection of MT. These improvements have been utilized mostly for analysis of MT in real biological samples; however, this study is focused on behavior of standard rabbit MT isoforms and therefore simple method was established. Sodium borate buffer (20 mM, pH 9.5) was used as a background electrolyte. Typical electropherograms of MT-1 (0.1 mg/mL) and MT-2 (0.1 mg/mL) are shown in Fig. 4A and B. Several signals are depicted in both figures. In the analysis of MT-2 isoform (Fig. 4B), the minor signals may be assigned to the MT-2 sub-isoforms. In the case of MT-1 signals (Fig. 4A), the origin of minor peaks may be associated with certain MT-like polypeptides, which are the most common impurities of MT standards. Subsequently, the separation of MT-1 and MT-2 mixture was successfully carried out under optimized condition (Fig. 4C). It is obvious that in spite of structural similarity (shown in Fig. 2) both isoforms behave differently, which is advantageous for their separation and detection. For all following calculations and analyses, only the height of major peaks –

Table 1. Bioinformatic data concerning the MT-1 and MT-2 isoforms and sub-isoforms (protein identification numbers (ID), name, number of amino acids (AAs), molecular mass, theoretical isoelectric points (p*I*)), data obtained from UniProtKB database using ProtParam tool

ID	Name	Number of AAs	Molecular mass (Da)	Theoretical p*I*
P18055	MT2A_RABIT	62	6083.1	8.24
P11957	MT1A_RABIT	61	6103.2	8.38
P80289	MT2B_RABIT	61	6104.1	8.23
P80290	MT2C_RABIT	62	6113.2	8.24
P80291	MT2D_RABIT	61	6173.3	8.38
P80292	MT2E_RABIT	61	6199.3	8.38
E2GJC7	E2GJC7_RABIT	61	5951.0	8.38

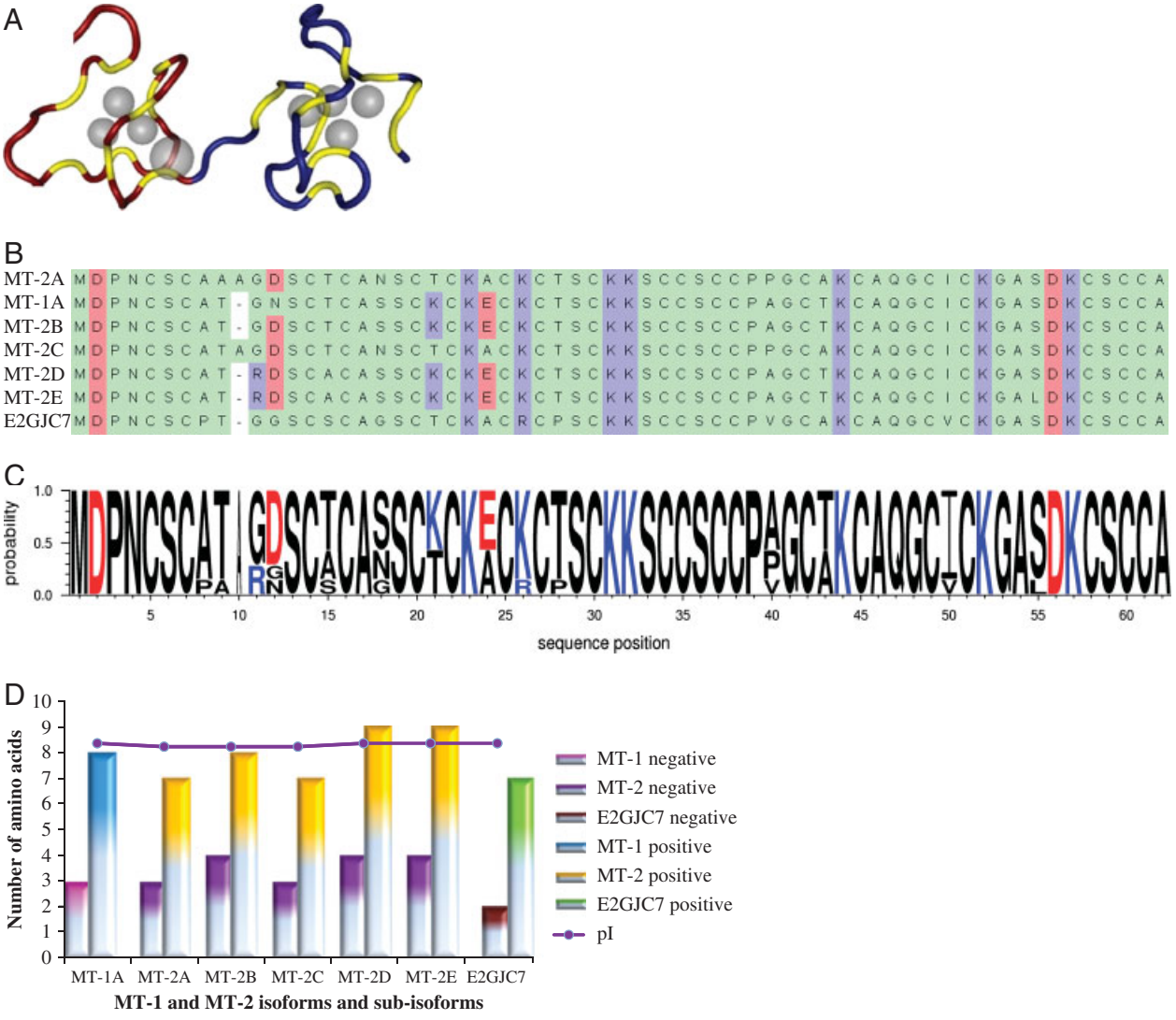

Figure 2. (A) Schematic structure of MT-based crystallography structure from UniProt data. (B) Alignment of amino acid sequences of MT-1 and MT-2 isoforms and sub-isoforms was performed using application created in the Matlab software with bioinformatic toolbox. (C) Representative logo – the probability of certain amino acid to occur in certain positions (the probability increases with the size of the letter). The change fraction was expressed in percentage of the ratio of each amino acid occurrence on certain position. Acidic and basic amino acids were color coded: neutral-black, acidic-red, basic-blue. Logo was created in professional application WebLogo3. (D) The number of acidic and basic amino acids and p*I* value of MT-1 and MT-2 isoforms and sub-isoforms from UniProt data.

which means MT-1 for MT-1 isoform and MT-2 for MT-2 isoform – was used. Calibration curves for each isoform exhibit very good linearity with correlation coefficients higher than 0.99 in the concentration range from 0.01 mg/mL (10 ng per injection as 1 μL) to 1.25 mg/mL (1250 ng per injection as 1 μL) (Fig. 4D). Figures of merit including limit of detection (LOD), limit of quantification (LOQ), migration time and signal relative standard deviation (RSD), correlation coefficient and linear regression equation are summarized in Table 2. Limits of detection estimated as 3 *S*/*N* according to Long and Winefordner [44] were 1 ng/μL and 0.1 ng/μL for MT-1 and MT-2, respectively. Relative standard deviations for migration times and signals were below 4%.

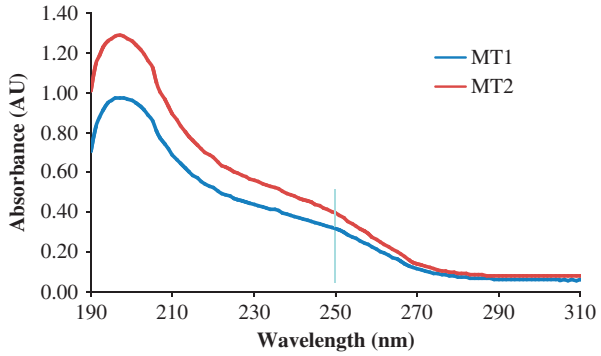

Figure 3. Absorption spectra of MT-1 and MT-2 in borate buffer (0.1 mg/mL) using double-beam spectrophotometer 210. The sample was placed into the low-volume (40 μl) quartz cell with optical path length of 1 cm at 25°C.

3.3 Condition-dependent structural changes

Protein denaturation is a complex process [45, 46] and its complete understanding requires taking into consideration numerous aspects such as net charge, protein structure, environmental conditions (e.g. electrolyte pH and concentration) as well as equilibrium of folded and unfolded protein form. In the case of CE analyses, also applied potentials have to be considered.

3.3.1 Thermal denaturation

Elevated temperature is one of the most commonly used approaches for protein denaturation [47]. It is employed as a sample pre-treatment method for extraction of thermally stable compounds from the complex real mixtures. MT is well known for its thermal stability and thermal denaturation belongs to the well-established techniques in MT determination [48]. The dependency of the CE signal on the heat treatment of the sample was studied by Kubo et al. [49]. The peak height of MT-1 of the standard MT-1 specimen decreased gradually from those of the non-heated specimen by thermal treatment at 100°C until 4 min, but the peak of

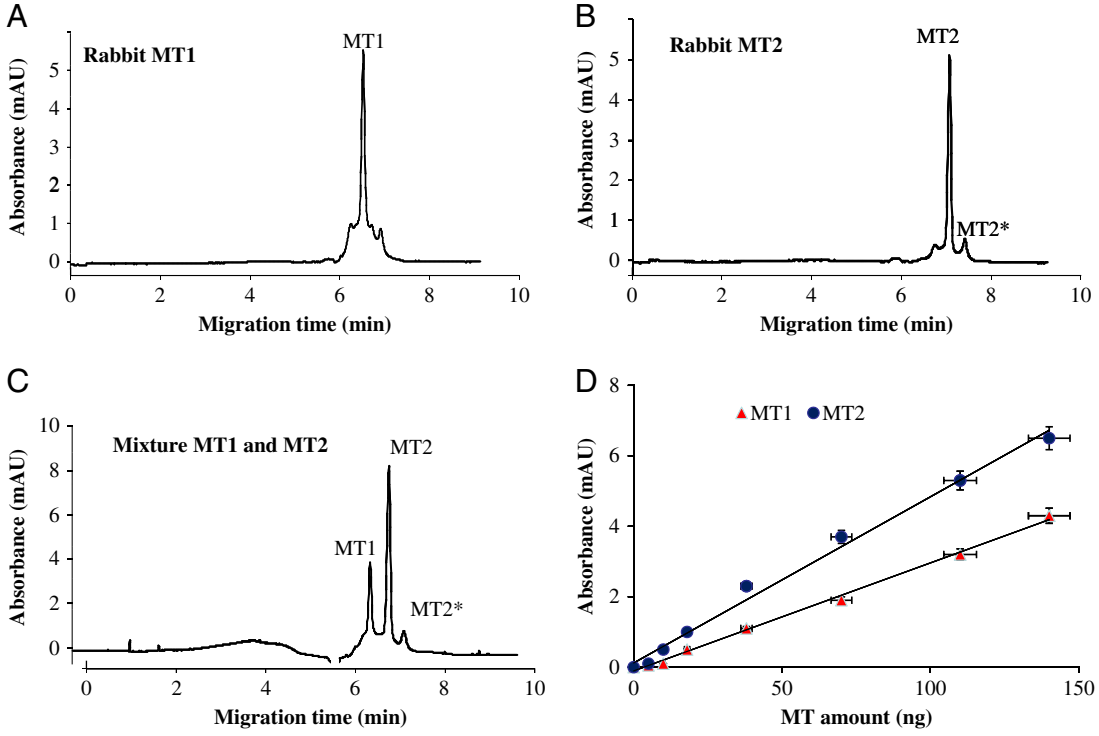

Figure 4. Typical electropherograms of (A) MT-1 0.12 mg/mL; 13 ng per inj. and (B) MT-2 0.12 mg/ml; 13 ng per inj. (C) Typical electropherogram of mixture of MT-1 and MT-2 (0.15 mg/mL; 16 ng per inj. (D) Calibration curves for MT-1 and MT-2 obtained in the range from 4.2 to 135.9 ng of MT on 1 μL injection. Experimental conditions were as follows: background electrolyte: 20 mM borate, pH 9.5, voltage: +15 kV, capillary: 50/57 cm, 75 μm, UV/VIS detection: 254 nm.

MT-2 did not decrease. The changes in the signals height were insignificant. In the present study, longer time of thermal treatment was selected and the background electrolyte was different from those used in the above-mentioned paper. CE signals of both isoforms increased linearly depending on the duration of the heat treatment at 99°C for various time intervals −0, 15, 30, 45 and 60 min (Fig. 5A). The increase was observed in both MT-1 as well as MT-2 within the range from 5 to 20 min of the treatment. The correlation coefficients of the measured dependencies as 0.9663 and 0.9853 were determined for MT-1 and MT-2, respectively. Electropherograms obtained are shown in Fig. 5B, where distinct changes in the signal heights are also indicated. This phenomenon suggests that the thermal treatment causes significant changes in the protein structure. Thermal denaturation is responsible for an irreversible precipitation leading to the aggregation of the denatured MT molecules and creating an undefined polymeric structure. The rate of the precipitation can be expressed as a slope of the linear regression of the time dependency curve recalculated on the MT concentration. The slope is expressed in ng of MT per length of denaturation (min). Thermal precipitation rate for MT-1 and MT-2 was determined as 1.1 and 0.9 ng of MT/min, respectively.

These results were compared with those obtained by DPV method (Fig. 5C). Electrochemical signal called Cat2 related to the concentration of MT in an electrochemical cell decreased with the increasing time of thermal treatment for

Table 2. Figures of merit (limit of detection (LOD), limit of quantification (LOQ), migration time and signal relative standard deviation (RSD), correlation coefficient and linear regression equation) obtained by capillary electrophoresis coupled with UV detector

	LOD (ng/μL) (S/N = 3)	LOQ (ng/μL) (S/N = 10)	Equation	R^2	Migration time RSD (%)	Signal RSD (%)
MT-1	1	3	$y = 0.0338x - 0.0022$	0.9968	3.2	0.6
MT-2	0.1	0.3	$y = 0.0486x + 0.0003$	0.9922	3.9	0.8

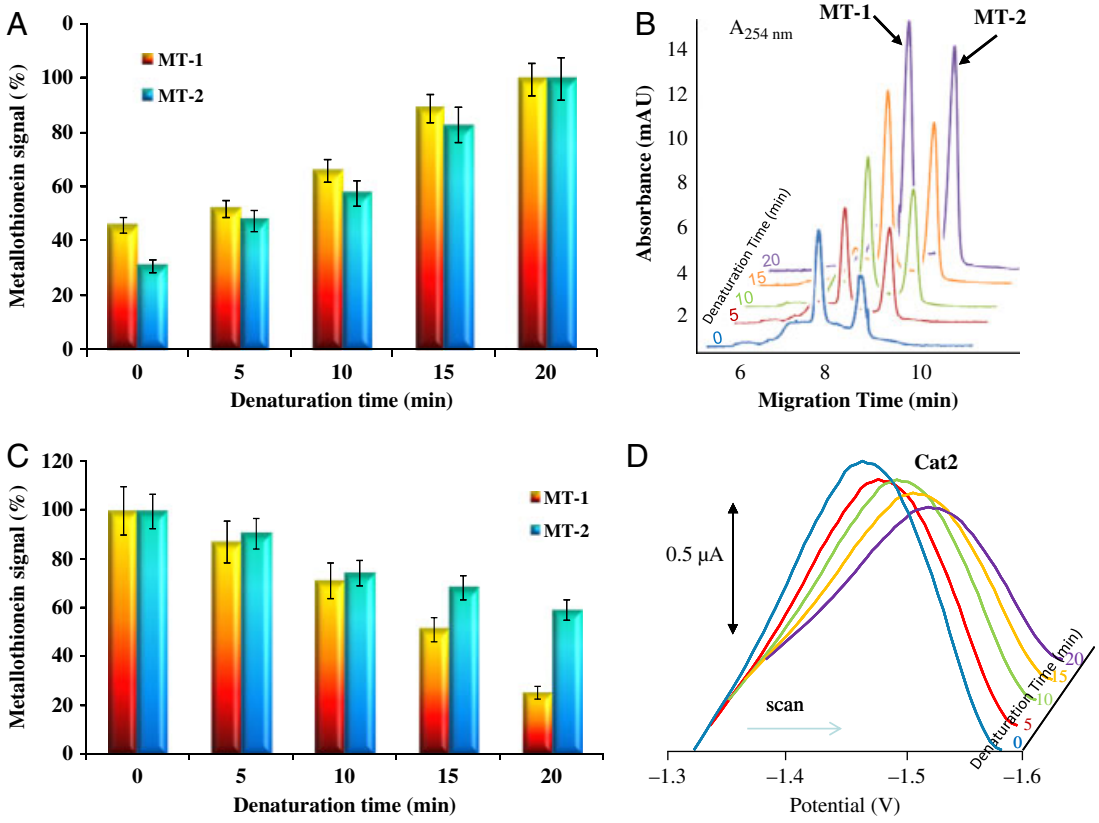

Figure 5. Thermal denaturation of MT-1 and MT-2 solution (protein concentration 0.1 mg/mL) at 99°C and their simultaneous detection using 254 nm. (A) Dependencies of MT-1 and MT-2 signal height on time of thermal treatment. Thermal denaturation of MT-1 and MT-2 solution (protein concentration 0.1 mg/mL) at 99°C and their detection using DPV Brdicka reaction. (B) Electropherograms of both thermal-treated isoforms. CE experimental conditions are the same as in Fig. 3. (C) Dependencies of Cat2 peak height of both MT isoforms on time of thermal treatment. (D) Catalytic peaks 2 (Cat2) of MT-2 isoform. DPV parameters were as follows: initial potential of −0.7 V, end potential of −1.75 V, modulation time 0.057 s, time interval 0.2 s, step potential 2 mV, modulation amplitude −250 mV, time of accumulation: 240 s.

both studied isoforms. The decreasing signals of MT-1 isoform during the thermal treatment are shown in Fig. 5D. The decrease in the signal observed by DPV is in agreement with CE results because the precipitation of the molecules may disable the interaction of electrochemically active amino acids (mostly cysteine) with the electrode [50–56]. Using the same calculation process, the precipitation rate for MT-1 and MT-2 was determined as 125 and 37.9 ng of MT/min, respectively. The precipitation rate is more sensitive in the case of electrochemistry, but one may take into account that electrochemical detection hardly distinguish between MT isoforms. Some precise isolation procedure such as paramagnetic particles must be coupled to enable MT isoform distinguishing.

The MT spectral behavior during the heat treatment was monitored also by stationary spectrophotometric method to support previously mentioned finding about precipitation rate of MT isoforms under thermal treatment. Significant spectral changes between heat-treated MT-1 solution and non-heated solution at the same concentration in the wavelength range 200–300 nm are clearly seen in Fig. 6A. On the other hand, in the case of MT-2 solution significant changes are observed only in the range of 190–220 nm. Only minor changes in spectral behavior of MT-2 solution are observed in the range from 220 to 300 nm comparing non-heated and heat-treated solutions (Fig. 6B). The time dependency of the absorbance at 214 nm is shown in Fig. 6C. The precipitation rate calculated at 214 nm was 0.34 ng of MT/min (MT-1) and 0.01 ng of MT/min (MT-2). Increasing trend can be observed in the case of MT-1, in contrary to the MT-2 which is exhibiting more stable behavior. However, for higher wavelength (254 nm) the increasing trend is observed in the case of both isoforms (Fig. 6D). The precipitation rate of 0.33 ng/min (MT-1) and 0.25 ng/min (MT-2) was calculated at 254 nm. Moreover, significant difference in the absorbance signal is apparent as expected.

3.3.2 Chemical denaturation

Another type of the treatment is a chemical denaturation. Commonly used denaturing agents include urea [57]. In this study, the effect of chemical denaturation by urea was experimentally tested to suggest the mechanism of MT behavior. Urea (7.5 M) was applied for various time intervals −0, 15, 30, 45 and 60 min. Due to the fact that all three tested methods revealed quite similar results, the structural changes caused by urea were followed primarily by CE. An increase in both isoforms signals with the increasing concentration of urea (Fig. 7A) was recorded. The 32 and 53% increase in the CE signal was observed for MT-1 and MT-2, respectively, as compared with signal heights at the beginning and at the end of chemical treatment. It is worth

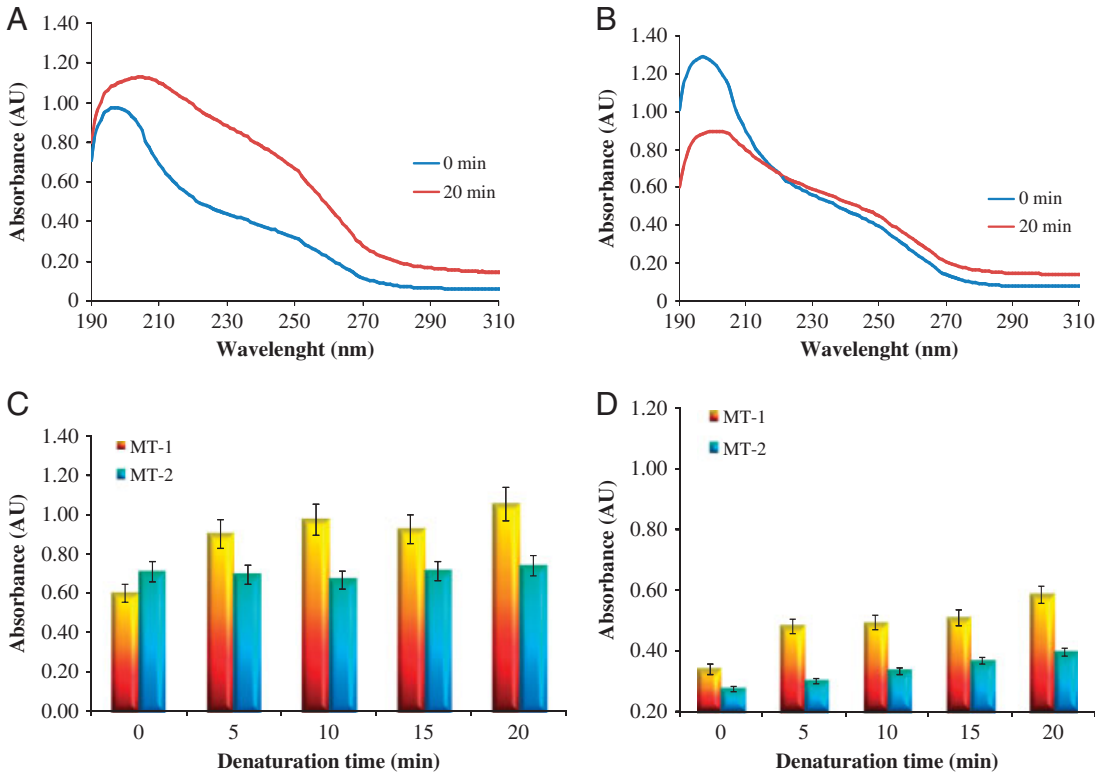

Figure 6. (A) Absorption spectra of non-heated and heat-treated MT-1 solution. (B) Absorption spectra of non-heated and heat-treated MT-2 solution. (C) Time dependency of the absorbance of both studied MT isoforms measured at 214 nm during the heat treatment at 99°C. (D) Time dependency of the absorbance of both studied MT isoforms measured at 254 nm during the heat treatment at 99°C. Experimental conditions: (0.1 mg/mL, time 20 min, temperature 99°C), other details see Fig. 4.

noticing that the absorbance of MT-2 isoform in the solution of 7.5 M urea increases during first 30 min more steeply in comparison to MT-1 signal. Contrary to the thermal denaturation providing comparable slope for both isoforms due to the higher impact of the temperature, chemical denaturation is much more sequence dependent and therefore providing significant difference between MT-1 and MT-2. The precipitation rate calculated from the linear regression for both isoforms provided the same value of 0.25 ng of MT/min. These results were in good agreement with DPV Brdicka reaction.

Based on the results obtained for both thermal and chemical denaturation it can be concluded that thermal denaturation is significantly more powerful and leads to precipitation independently on the protein sequence. On the other hand, chemical denaturation by 7.5 M urea solution differs significantly for each isoform especially in the first 30 min of the incubation. Also, the precipitation rate is

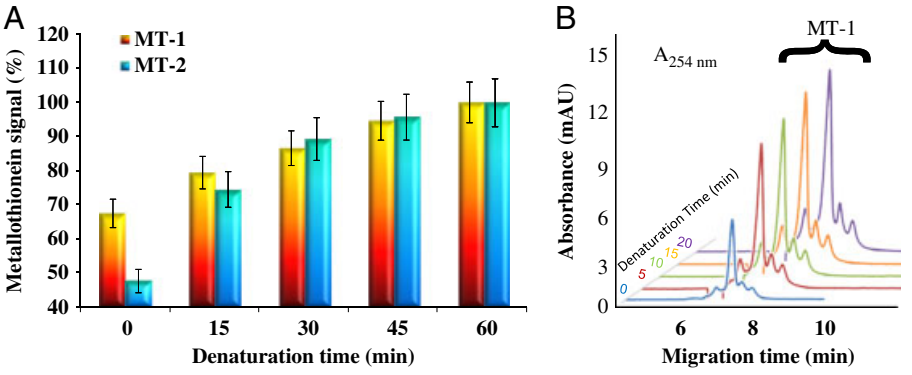

Figure 7. Chemical denaturation. (A) Time dependency of MT-1 and MT-2 denaturation by 7.5 M urea measured by CE (0.1 mg/mL). (B) Electropherograms of MT-1 in the presence of 7.5 M urea. Other experimental conditions are the same as in Fig. 4.

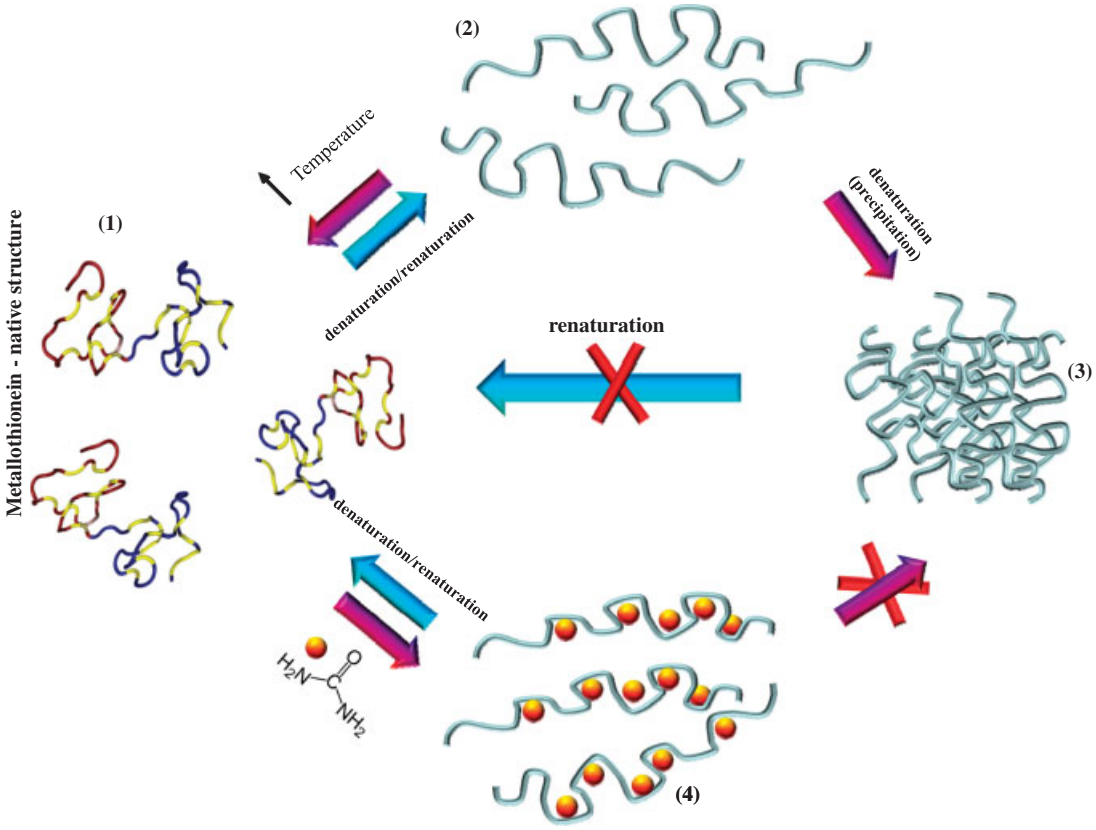

Figure 8. Suggested model of MT behavior under studied conditions (temperature of 99°C and/or 7.5 M urea). (1) MT in native structure. Both MT isoforms are denatured under physical (2) and/or chemical (4) treatment. However, the thermal treatment causes irreversible changes due to precipitation of denatured protein structures (3). In the case of chemical treatment, urea is probably bounded in the denatured structure of proteins like sodium dodecyl sulfate, which prevents proteins to precipitate (4). Based on this, chemical, but not physical, treatment is reversible.

lower for chemical denaturation confirming the slower mechanism of the denaturation based on the interaction of urea molecules with the unfolded molecule disabling the intermolecular reaction and precipitation. Therefore, the protein molecules restore the original structure when urea is removed from the solution. In the case of thermal precipitation, the aggregates are irreversible and stable. Based on the results, a model of MT behavior under studied conditions was suggested in Fig. 8. The thermal treatment causes irreversible changes due to precipitation of denatured protein structures. In the case of chemical treatment, urea is probably bounded in the denatured structure of proteins like sodium dodecyl sulfate, which prevents proteins to precipitate [58, 59]. Based on this, chemical treatment is reversible, but physical not.

4 Concluding remarks

It has been recently published that MT is involved not only in storage and detoxification of heavy metals, but it has also a regulation function. Its connection with some tumor processes is very likely. Therefore, methods distinguishing of MT isoforms are needed. The present paper shows advantages of capillary electrophoresis as a tool for this purpose. However, not only concentration of protein, but also structural state (native or denaturated) is of great importance. It is a protein's tertiary, native (folded) structure that makes it capable of performing its biological function. Native (folded) and denaturated (unfolded) proteins can be detected by circular dichroism and by nuclear magnetic resonance. However, these techniques are expensive and laborious. We show in this study that capillary electrophoresis coupled with UV–VIS detector can be used for studying of structural changes in low molecular mass protein (MT) and also for defining the dynamics of these changes. The optimized method and presented application can be used in the following research for studying of isoforms of various proteins and for finding their structural differences.

Financial support from the following projects CEITEC CZ.1.05/1.1.00/02.0068, RECAMT GA AVIAA401990701 and NANOSEMED GA AVKAN208130801 is highly acknowledged. The authors wish to express their thanks to Petr Majzlik for technical assistance.

The authors have declared no conflict of interest.

5 References

[1] Coyle, P., Philcox, J. C., Carey, L. C., Rofe, A. M., *Cell. Mol. Life Sci.* 2002, *59*, 627–647.

[2] Dunn, M. A., Blalock, T. L., Cousins, R. J., *Proc. Soc. Exp. Biol. Med.* 1987, *185*, 107–119.

[3] Hamer, D. H., *Annu. Rev. Biochem.* 1986, *55*, 913–951.

[4] Masters, B. A., Quaife, C. J., Erickson, J. C., Kelly, E. J., Froelick, G. J., Zambrowicz, B. P., Brinster, R. L., Palmiter, R. D., *J. Neurosci.* 1994, *14*, 5844–5857.

[5] Moffatt, P., Seguin, C., *DNA Cell Biol.* 1998, *17*, 501–510.

[6] Quaife, C. J., Findley, S. D., Erickson, J. C., Froelick, G. J., Kelly, E. J., Zambrowicz, B. P., Palmiter, R. D., *Biochemistry* 1994, *33*, 7250–7259.

[7] Beattie, J. H., Bremner, I., in: Roussel, A. M., Anderson, R. A., Favrier, A.E. (Eds.), *Trace elements in man and animals*, Springer, Vol. 10, 200, pp. 961–967.

[8] Miles, A. T., Hawksworth, G. M., Beattie, J. H., Rodilla, V., *Crit. Rev. Biochem. Mol. Biol.* 2000, *35*, 35–70.

[9] Beattie, J. H., Bremner, I., in: Collery, P., Bratter, P., deBratter, V. N., Khassanova, L., Etienne, J. C. (Eds.), *Metal Ions in Biology and Medicine*, French & European Pubns, Vol. 5, 1998, pp. 117–127.

[10] Eckschlager, T., Adam, V., Hrabeta, J., Figova, K., Kizek, R., *Curr. Protein Pept. Sci.* 2009, *10*, 360–375.

[11] Krizkova, S., Fabrik, I., Adam, V., Hrabeta, P., Eckschlager, T., Kizek, R., *Bratisl. Med. J.* 2009, *110*, 93–97.

[12] McGee, H. M., Woods, G. M., Bennett, B., Chung, R. S., *Photochem. Photobiol. Sci.* 2010, *9*, 586–596.

[13] Pedersen, M. O., Larsen, A., Stoltenberg, M., Penkowa, M., *Prog. Histochem. Cytochem.* 2009, *44*, 29–64.

[14] Krizkova, S., Adam, V., Eckschlager, T., Kizek, R., *Electrophoresis* 2009, *30*, 3726–3735.

[15] Krizkova, S., Adam, V., Kizek, R., *Electrophoresis* 2009, *30*, 4029–4033.

[16] Krizkova, S., Blahova, P., Nakielna, J., Fabrik, I., Adam, V., Eckschlager, T., Beklova, M., Svobodova, Z., Horak, V., Kizek, R., *Electroanalysis* 2009, *21*, 2575–2583.

[17] Krizkova, S., Masarik, M., Eckschlager, T., Adam, V., Kizek, R., *J. Chromatogr. A* 2010, *1217*, 7966–7971.

[18] Adam, V., Fabrik, I., Eckschlager, T., Stiborova, M., Trnkova, L., Kizek, R., *Trac-Trends Anal. Chem.* 2010, *29*, 409–418.

[19] Ryvolova, M., Krizkova, S., Adam, V., Beklova, M., Trnkova, L., Hubalek, J., Kizek, R., *Curr. Anal. Chem.* 2011.

[20] Minami, T., Matsubara, H., Ohigashi, M., Otaki, N., Kimura, M., Kubo, K., Okabe, N., Okazaki, Y., *J. Chromatogr. B* 1996, *685*, 353–359.

[21] Virtanen, V., Bordin, G., *J. Liq. Chromatogr. Relat. Technol.* 1998, *21*, 3087–3098.

[22] Virtanen, V., Bordin, G., Rodriguez, A. R., *J. Chromatogr. A* 1996, *734*, 391–400.

[23] Minami, T., Kubo, K., Ichida, S., *J. Chromatogr. B* 2002, *779*, 211–219.

[24] Minami, T., Ichida, S., Kubo, K., *J. Chromatogr. B* 2002, *781*, 303–311.

[25] Kawata, T., Nakamura, S., Nakayama, A., Fukuda, H., Ebara, M., Nagamine, T., Minami, T., Sakurai, H., *Biol. Pharm. Bull.* 2006, *29*, 403–409.

[26] Alvarez-Llamas, G., de la Campa, M. R. F., Sanz-Medel, A., *Anal. Chim. Acta* 2001, *448*, 105–119.

[27] Prange, A., Schaumloffel, D., Bratter, P., Richarz, A. N., Wolf, C., *Fres. J. Anal. Chem.* 2001, *371*, 764–774.

[28] Schaumloffel, D., Prange, A., Marx, G., Heumann, K. G., Bratter, P., *Anal. Bioanal. Chem.* 2002, *372*, 155–163.

[29] Petrlova, J., Potesil, D., Mikelova, R., Blastik, O., Adam, V., Trnkova, L., Jelen, F., Prusa, R., Kukacka, J., Kizek, R., *Electrochim. Acta* 2006, *51*, 5112–5119.

[30] Adam, V., Baloun, J., Fabrik, I., Trnkova, L., Kizek, R., *Sensors* 2008, *8*, 2293–2305.

[31] Fabrik, I., Krizkova, S., Huska, D., Adam, V., Hubalek, J., Trnkova, L., Eckschlager, T., Kukacka, J., Prusa, R., Kizek, R., *Electroanalysis* 2008, *20*, 1521–1532.

[32] Gascuel, O., *Mol. Biol. Evol.* 1997, *14*, 685–695.

[33] Muller, T., Vingron, M., *J. Comput. Biol.* 2000, *7*, 761–776.

[34] Crooks, G. E., Hon, G., Chandonia, J. M., Brenner, S. E., *Genome Res.* 2004, *14*, 1188–1190.

[35] Kagi, J. H. R., Schaffer, A., *Biochemistry* 1988, *27*, 8509–8515.

[36] Trnkova, L., Kizek, R., Vacek, J., *Bioelectrochemistry* 2002, *56*, 57–61.

[37] Shen, J. C., Huang, Z. Y., Zhuang, Z. X., Wang, X. R., Lee, F. S. C., *Appl. Organomet. Chem.* 2005, *19*, 140–146.

[38] Virtanen, V., Bordin, G., *Anal. Chim. Acta* 1998, *372*, 231–239.

[39] Virtanen, V., Bordin, G., *Anal. Chim. Acta* 1999, *402*, 59–66.

[40] Virtanen, V., Bordin, G., Rodriguez, A. R., *J. Chromatogr. A* 1996, *734*, 391–400.

[41] Wilhelmsen, T. W., Hansen, B. H., Holten, V., Olsvik, P. A., Andersen, R. A., *J. Chromatogr. A* 2004, *1051*, 237–245.

[42] Beattie, J. H., Richards, M. P., *J. Chromatogr. A* 1995, *700*, 95–103.

[43] Nakamura, S., Kawata, T., Nakayama, A., Kubo, K., Minami, T., Sakurai, H., *Biochem. Biophys. Res. Commun.* 2004, *320*, 1193–1198.

[44] Long, G. L., Winefordner, J. D., *Anal. Chem.* 1983, *55*, A712–A724.

[45] Piaggio, M. V., Peirotti, M. B., Deiber, J. A., *Electrophoresis* 2007, *28*, 2223–2234.

[46] Kim, J. Y., Ahn, S. H., Kang, S. T., Yoon, B. J., *J. Colloid Interface Sci.* 2006, *299*, 486–492.

[47] Myers, J. K., Pace, C. N., Scholtz, J. M., *Protein Sci.* 1995, *4*, 2138–2148.

[48] Erk, M., Ivankovic, D., Raspor, B., Pavicic, J., *Talanta* 2002, *57*, 1211–1218.

[49] Kubo, K., Sakita, Y., Minami, T., *Analysis* 2000, *28*, 366–369.

[50] Potesil, D., Mikelova, R., Adam, V., Kizek, R., Prusa, R., *Protein J.* 2006, *25*, 23–32.

[51] Huska, D., Adam, V., Zitka, O., Kukacka, J., Prusa, R., Kizek, R.,*Electroanalysis* 2009, *21*, 536–541.

[52] Zitka, O., Horna, A., Stejskal, K., Zehnalek, J., Havel, L., Zeman, L., Kizek, R., *Acta Chim. Slov.* 2007, *54*, 68–73.

[53] Zitka, O., Krizkova, S., Huska, D., Adam, V., Hubalek, J., Eckschlager, T., Kizek, R., *Electrophoresis* 2011, *32*, 857–860.

[54] Ostatna, V., Cernocka, H., Palecek, E., *J. Am. Chem. Soc.* 2010, *132*, 9408–9413.

[55] Ostatna, V., Kuralay, F., Trnkova, L., Palecek, E., *Electroanalysis* 2008, *20*, 1406–1413.

[56] Ostatna, V., Palecek, E., *Electrochim. Acta* 2008, *53*, 4014–4021.

[57] Greene, R. F., Pace, C. N., *J. Biol. Chem.* 1974, *249*, 5388–5393.

[58] Schagger, H., Vonjagow, G., *Anal. Biochem.* 1987, *166*, 368–379.

[59] Pitt-Rivers, R., Impiombato, F. S. A., *Biochem. J.* 1968, *109*, 825–830.

